 MCB, vol.3, no.3, pp.89-94, 2006

Molecular Dynamics Simulation of the Size Effect of Carbon Nanotubes on the Bulk Modulus of a Lipid Bilayer

Yong Gan* **and Zhen Chen***,†

Abstract: Due to their nanoscale size and special features, carbon nanotubes could enter the human body via certain way. The growing use of carbon nanotubes in practical applications, hence, prompts a necessity to study the potential health risks of carbon nanotubes. A numerical study is performed in this paper to investigate the size effect of carbon nanotubes on the bulk modulus of a lipid bilayer by using the constant surface tension molecular dynamics simulation procedure. It is found that the size effect is not monotonic with the increase of nanotube length. An explanation is given on the basis of the atomic interaction between the nanotube and bilayer involved in the model system.

1 Introduction

Carbon nanotubes have been attracting lots of interests since their discovery in 1991 (1), due to their extraordinary mechanical strength, exceptional electrical conductivity, special heat conduction and optical features, etc. Because of their nano-scale size, however, carbon nanotubes could enter the blood stream through the lungs and possibly through the skin, and probably enter the brain directly via olfactory nerves. Furthermore, carbon nanotubes are deemed to be one promising carrier for the target delivery of drugs, proteins and other biomolecules due to their good biocompatibility, low cytotoxicity, unique physicochemical properties and large inner volume (2). In a word, there might exist various ways for carbon nanotubes to enter a human body. Once in the body, carbon nanotubes, unlike larger particles that can be trapped and removed by various protective mechanisms, are able to move practically unhindered throughout the entire body with the blood stream. As can be found from the open literature, however, little is currently known about the potential health risks of manufactured nanomaterials, including carbon nanotubes.

* Department of Civil and Environmental Engineering, University of Missouri-Columbia, Columbia, MO 65211, USA

† Corresponding author, Email: chenzh@missouri.edu

On the other hand, the interest in mechanical forces as biological regulators is recently growing. Mechanical forces are recognized as an important factor for the development and function of the heart and lung, the growth of skin and muscle, the maintenance of cartilage and bone, and the etiology of many debilitating diseases, including hypertension, osteoporosis, asthma and heart failure. It is also revealed that the behaviors required for developmental control, such as growth, differentiation, polarity and motility, are all affected by the physical distortion of cells (3). Cell membranes define the inside and outside of a cell. They serve some indispensable functions for life. For example, cell membranes behave as one barrier to prevent molecules generated inside the cell from leaking out and unwanted molecules from diffusing in; they also contain transport systems that allow specific molecules to be taken up and unwanted compounds to be removed from the cell (4). To fully understand how cells function, therefore, it is necessary to investigate the physical deformations of cell membranes subjected to the mechanical forces. Simulation of a membrane at macroscopic spatial and temporal scales can now be fulfilled by treating the membrane as a continuum without biological detail (5, 6, among others). To solve the equations of motion, however, a constitutive model that relates stresses to strains must be known in advance. The coefficients of the constitutive relation, such as bulk modulus, determine the cell responses to the mechanical forces.

Because it is easy for carbon nanotubes to be absorbed into the human body, the mechanical properties of the cell membrane might change due to the interaction between the nanotube and membrane. Phospholipid bilayers are abundant in all biological membranes (4), and have served as a model of the biological membrane in a large number of studies (7-11, among others). So far, all simulations and experiments designed to find the material properties of membranes have involved the pure bilayer only. With the increased potential of practical applications of carbon nanotubes, efforts are required

to study the influence of carbon nanotubes on the mechanical properties of the bilayers. Molecular dynamics (MD) simulation has proved to be an efficient tool for investigating the material properties of lipid bilayers (9-11, among others). In this paper, MD simulations are performed to investigate the size effect of carbon nanotubes on the bulk modulus of a palmitoyloleoylphosphatidylcholine (POPC) bilayer. With the use of the controlled constant surface tensions, the simulated system composed of a pure bilayer and one carbon nanotube of various sizes is subjected to the stresses on the surface plane of the bilayer. The bulk modulus is then obtained by examining the surface area of the bilayer under the imposed forces.

The remaining of the paper is organized as below. The continuum-level bulk modulus of a membrane is discussed first. Then the setup of the MD model and details of MD simulations are given. The simulation results for the bulk modulus of a POPC bilayer and concluding remarks are presented in the final section.

2 Simulation methods

2.1 Bulk modulus of a membrane

As discussed by E. Evans and D. Needham (12), deformations of thin membranes are described by simple shape changes of the membrane surface, i.e., area change, surface shear and bending change, which are related to the stresses via the constitutive relations. For a membrane placed in the $x-y$ plane with thickness in the z direction, the mean tension, σ, is proportional to the fractional area dilation or contraction, i.e.

$$\sigma = K\alpha \tag{1}$$

where $\sigma = (\sigma_{xx}+\sigma_{yy})/2$ is the mean tension with σ_{xx} and σ_{yy} being the components of the stress tensor in the x and y directions, respectively, $\alpha = (A-A_0)/A_0$ is the fractional area dilation or contraction with A_0 and A respectively denoting the original and current surface area of the membrane, and K is the bulk modulus. Conceptually, the bulk modulus is a proportionality constant relating surface area changes to stresses.

2.2 Surface tension

In MD simulations, the pressure tensor of the simulated system is computed from all the kinetic energies and pairwise interparticle interactions as follows (13):

$$P_{\alpha\beta} = \frac{1}{V}\left(\sum_i v_{i\alpha}v_{i\beta}\Big/ m_i + \sum_i\sum_{j>i} r_{ij\alpha}f_{ij\beta}\right) \tag{2}$$

where α and β denote the directions of x, y and z, $v_{i\alpha}$ and $v_{i\beta}$ are the momentums of particle i in α and β directions, respectively, m_i is the mass of particle i, $r_{ij\alpha}$ is the component of the position vector between particle i and j in the α direction, $f_{ij\beta}$ is the component of the force vector on particle i due to j in the β direction, and V is the volume of the simulated system. According to Newton's First Law, the stress component applied to the simulated system is the negative of the pressure tensor component, namely

$$\sigma = -\mathbf{P} \tag{3}$$

The surface tension, γ, is related to the pressure tensor (14) and given by

$$\gamma = \left\langle L_z \cdot \left(P_{zz} - \frac{1}{2}P_{xx} - \frac{1}{2}P_{yy}\right)\right\rangle \tag{4}$$

in which L_z and P_{zz} are respectively the length of the simulation box and component of the pressure tensor normal to the membrane surface, P_{xx} and P_{yy} are the tangential components of the pressure tensor, and the angular brackets denote an average. It can be found from Eq. (4) that the tangential pressures smaller than the pressure normal to the surface will lead to positive values of surface tension. The MD simulations are performed with the surface tension being kept constant at specified values. The mean tension and the corresponding surface area can be obtained by monitoring the pressure tensor and the dimensions of the simulation box. As a result, the bulk modulus can be found by fitting the data with the use of a linear regression approach.

2.3 Model formulation and simulation procedure

The membrane studied here is a patch of POPC bilayer which is constructed using the membrane-building tool of the molecular graphic program VMD (15). Figure 1 shows the molecular images of the simulated system created with VMD. The bilayer contains 128 POPC molecules with 64 lipid molecules per layer and is hydrated by 6760 water molecules. The initial ensemble is obtained from a 2-ns NPAT (i.e., constant number of

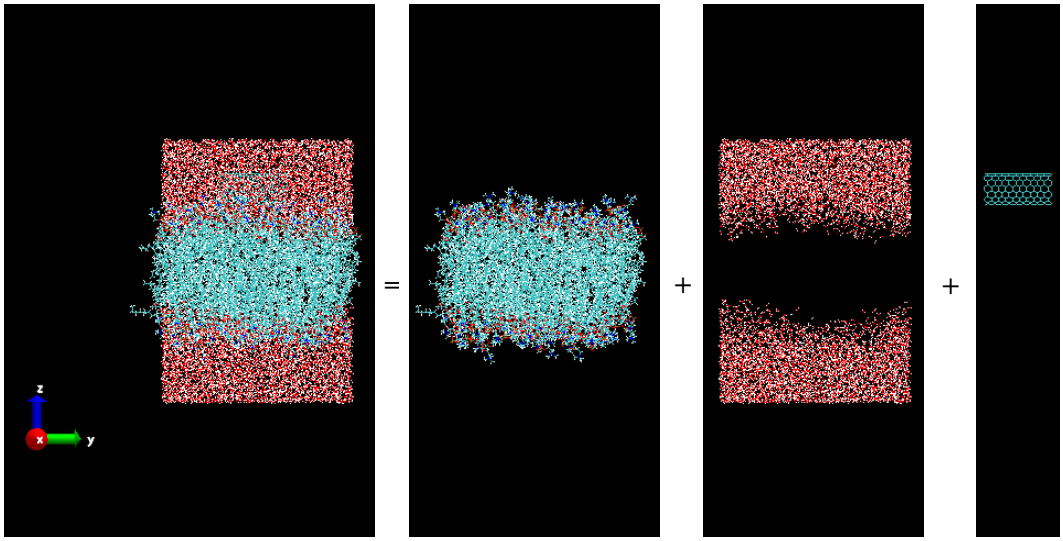

Figure 1 : The simulation system containing lipids, water and a single-walled carbon nanotube: (a) The whole system; (b) POPC bilayer; (c) Water layer; (d) Carbon nanotube

atoms, constant normal pressure, and fixed surface area and temperature) simulation, in which the surface area per lipid (i.e., surface area of the bilayer divided by the number of lipid molecules per layer) and the pressure tensor component normal to the membrane surface are kept constant at 64 $Å^2$ and 1 atm, respectively. The first 1 ns NPAT simulation is undertaken to equilibrate the system merely containing the lipid bilayer and water molecules. After the 1 ns equilibration, a single-walled carbon nanotube (SWNT) of various lengths is inserted into the system, and then another 1 ns NPAT simulation is performed. To investigate the size effect of the SWNTs on the bulk modulus of the bilayer, seven SWNTs of (8, 8) armchair type are employed. The length of nanotubes starts at 5 Å and increases with an increment of 5 Å. Hence, the longest nanotube is 35 Å in length. In the nanotubes, all the carbon atoms have a zero charge. The nanotube is oriented along the y-axis of the system. The centroid of the nanotubes has the same x and y coordinates as the mass center of the bilayer, and the centroid is located 1 nm above the upper surface of the bilayer at $z = z_c$ where z_c is the average z coordinate of phosphorus atoms in the upper lipid layer. In addition, three carbon atoms in the nanotubes are fixed to prevent the orientation change of nanotubes during the MD simulations.

All the MD simulations are conducted using the parallel molecular dynamics program NAMD (16). The CHARMM22 force field is employed for the lipids and SWNTs (17), and the parameters for the carbon atoms in the SWNTs are those of type *CA* designed for benzene in the CHARMM22 potential (18). The cutoff of 12Å is chosen for the van der Waals (VDW) interactions and the particle mesh Ewald method (PME) (19) for the full electrostatics. The TIP3P model (20) is used for water molecules. A timestep of 2 fs is employed. The temperature is maintained at 323K by means of Langevin dynamics. The hybrid Nosé-Hoover Langevin piston method is used to maintain the pressure and surface tensions at the given values (21). The MD simulations at surface tensions of 40, 50, 60, 70, and 80 dyn/cm are performed for each model system. During the constant surface tension MD simulations, a fully flexible cell is employed with the z dimension varied to maintain P_{zz}=1 atm, and the x and y dimensions adjusted to maintain the desired surface tension γ. Each constant surface tension simulation takes 3 ns in time and all simulations are carried out at the National Center for Supercomputing Applications.

3 Results and discussion

It can be observed from Eq. (1) that $A = A_0$ leads to zero mean tension. The value of A_0 for each model system is not known in advance. The bulk modulus of the bilayer, thus, could not be determined by fitting the paired data of (σ, α) due to the unavailable value of α. Substituting

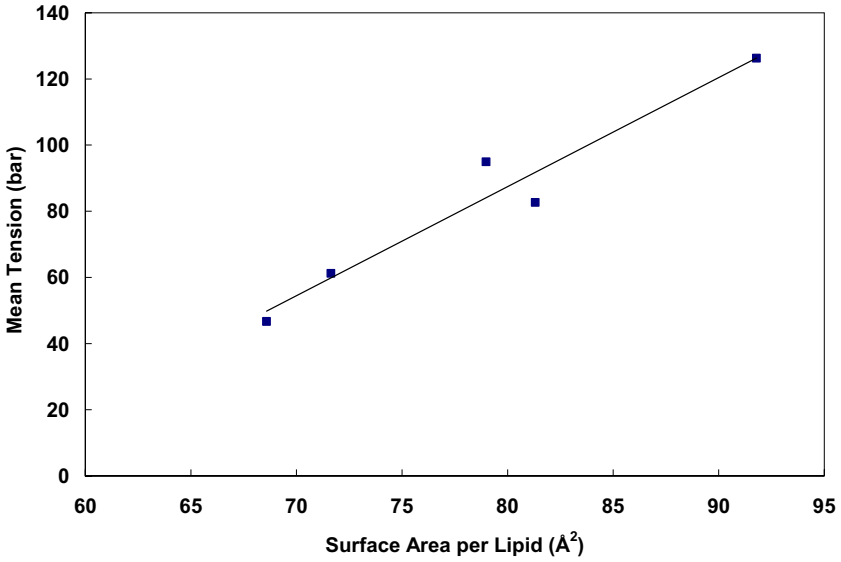

(a)

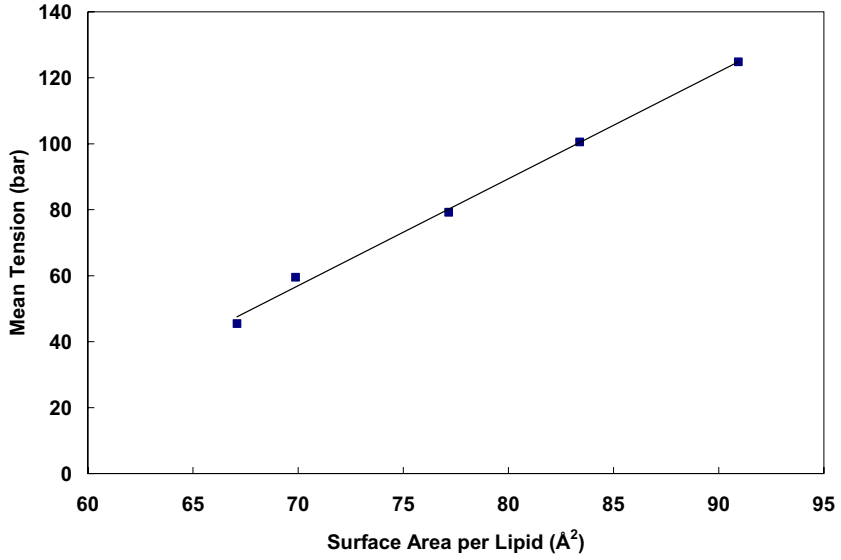

(b)

Figure 2 : Mean tension vs surface area per lipid: (a) a system containing 5 Å long carbon nanotube; (b) a system containing 10 Å long carbon nanotube

$\alpha = (A - A_0)/A_0$ into Eq. (1) with $\widehat{\beta} = K/A_0$ and $\widehat{\alpha} = K$ yields

$$\sigma = \widehat{\beta} A - \widehat{\alpha} \tag{5}$$

Each constant surface tension simulation could give a mean tension σ and the corresponding surface area A. Thus, a set of five paired data could be obtained for each model system. The bulk modulus of the bilayer could then be determined by fitting the paired data $\{(\sigma_i, A_i);\ i = 1, 2, 3, \ldots, 5\}$ with the use of the standard least squares method. The average values over the last 500 ps MD simulations are used for the data analysis. Figure 2 plots the mean tension vs the surface area per lipid and the least squares line for the systems containing 5 Å and 10 Å long carbon nanotubes. Table 1 demonstrates the size effect of SWNTs on the bulk modulus of the POPC bilayer.

The resistance of a bilayer to external forces origi-

Table 1 : Calculated bulk modulus of the lipid bilayer

Simulation number	Length of the SWNT (Å)	Bulk modulus (10^7 Nm^{-2})
1	5	1.76
2	10	1.70
3	15	1.71
4	20	1.76
5	25	1.98
6	30	1.82
7	35	1.75

nates from the nonbonded interactions between lipid molecules. The CHARMM22 force field describes the interactions between nonbonded atoms by Coulombic and Lennard-Jones (LJ) potentials (16), which are respectively expressed as

$$E_{coul} = \frac{q_i q_j}{\varepsilon_l r_{ij}} \tag{6}$$

$$E_{LJ} = \varepsilon \left[\left(\frac{R_{\min}}{r_{ij}} \right)^{12} - \left(\frac{R_{\min}}{r_{ij}} \right)^{6} \right] \tag{7}$$

where E_{coul} is the Coulomb potential, E_{LJ} is the Lennard-Jones energy, ε_l is the effective dielectric constant, q_i and q_j are respectively partial atomic charges on atom i and j, ε is the Lennard-Jones well depth, $R_{\min}$ is the distance at the Lennard-Jones minimum, and r_{ij} is the distance between atoms i and j. As can be seen from Eqs. (6) and (7), the nonbonded forces are only dependent on the atomic distance with given atom types and atomic charges. Therefore, the essence of the surface area change of a bilayer is to adjust nonbonded forces between lipid molecules to resist the imposed forces on the surface plane of the bilayer.

As far as the simulated systems are concerned, the carbon nanotube affects the ability of the bilayer to resist external forces through the interaction between the nanotube and the bilayer. This interaction is governed only by the LJ potential because carbon atoms in the nanotubes are neutrally charged. For a short nanotube, the interaction between the nanotube and the bilayer is much weaker than that between lipid molecules. Hence, it can be observed from Table 1 that the bulk modulus of the bilayer is almost the same for simulations 1-4. The increase of carbon atoms with the nanotube length would lead to a stronger interaction between the nanotube and the bilayer. As shown in Fig. 3, however, the LJ force includes attraction and repulsion. In the present constant surface tension MD simulations, the bilayer is subjected to the external tension on the surface plane. The external tension could be partially counteracted by the attraction acted on the bilayer due to the nanotube. In other words, the attraction strengthens the resistance of the bilayer to the external tension, while the repulsion would reduce such resistance. Due to the combining effects of attraction and repulsion between the nanotube and bilayer, therefore, the bulk modulus of the bilayer can not monotonically increase with the nanotube length, as demonstrated by the results of simulations 5-7.

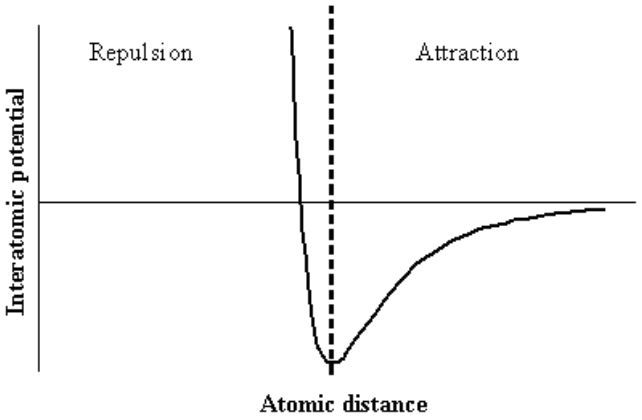

Figure 3 : Lennard-Jones potential

In summary, it can be found from this MD study that carbon nanotubes of various sizes do affect the bulk modulus of the bilayer although the difference is not pronounced. It is still unknown, however, whether any small change in the material properties would induce a significant variation of cell functions. It should be noted that we have

only considered the size effect due to the length change of the SWNTs in this work. Many other aspects of carbon nanotubes remain to be considered in the future work to better understand their effects on the cell functions.

Acknowledgement: This work was sponsored in part by the NSF-NIRT program under Grant No. 0304472, and by the Program for Changjiang Scholars and Innovative Research Teams (PCSIRT) in the NSFC under Grant No. 10421002, and the National Key Basic Research Special Foundation of China under Grant No. 2005CB321704. The authors also acknowledge the computing time provided by Development Allocation Committee grant MSS060005T.

References

1. Iijima, S. (1991) *Nature* **354**, 56-58.
2. Xu, Z., Zeng, Q., Lu, G., & Yu, A. (2006) *Chem. Eng. Sci.* **61,** 1027-1040.
3. Ingber, D.E. (2003) *J. Cell Sci.* **116**, 1397-1408.
4. Berg, J.M., Tymoczko, J.L., & Stryer L. (2002) in *Biochemistry* (W.H. Freeman, New York), pp. 319-344.
5. York, A., Sulsky, D., & Schreyer, H. (1999) *Int. J. Num. Meth.* **44**,1429-1456.
6. Koivurova, H., & Pramila, A. (1997) *Comp. Mech.* **20**, 573-581.
7. Solletti, J.M., Botreau, M., Sommer, F., Brunat, W.L., Kasas, S., Tran Minh Duc, & Celio, M.R. (1996) *Langmuir* **12**, 5379-5386.
8. Grandbois, M., Clausen-Schaumann, H., & Gaub, H. (1998) *Biophys. J.* **74**, 2398-2404.
9. Feller, S.E., & Pastor, R.W. (1999) *J. Chem. Phys.* **111**, 1281-1287.
10. Shinoda, W., Namiki, N., & Okazaki, S. (1997) *J. Chem. Phys.* **106**, 5731-5743.
11. Ayton, G., Smondyrev, A.M., Bardenhagen, S.G., McMurtry, P. & Voth, G.A. (2002) *Biophys. J.* **82**, 1226-1238.
12. Evans, E., & Needham, D. (1987) *J. Phys. Chem.* **91**, 4219-4228.
13. Allen, M., & Tildesley, D. (1987) In *Computer simulation of liquids* (Oxford University Press, New York), pp. 33-70.
14. Zhang, Y., Feller, S.E., Brooks, B.R., & Pastor, R.W. (1995) *J. Chem. Phys.* **103**, 10252-10266.
15. Humphrey, W., Dalke, A., & Schulten, K. (1996) *J. Mol. Graph.* **14**, 33-38.
16. Kalé, L., Skeel, R., Bhandarkar, M., Brunner, R., Gursoy, A, Krawetz, N., Phillips, J., Shinozaki, A., Varadarajan, K., & Schulten, K. (1999) *J. Comput. Phys.* **151**, 283-312.
17. MacKerell, A.D., Jr., Bashford, D., Bellott, M., Dunbrack, R.L., Jr., Evanseck, J., Field, M.J., Fischer, S., Gao, J., Guo, H., Ha, S., et al. (1998) *J. Phys. Chem. B.* **102**, 3586-3616.
18. Zhu, F., & Schulten, K. (2003) *Biophys. J.* **85**, 236–244.
19. Essmann, U., Perera, L., Berkowitz, M.L., Darden, T., Lee, H., & Pedersen, L.G. (1995) *J. Chem. Phys.* **103**, 8577–8593.
20. Jorgensen, W.L., Chandrasekhar, J., Madura, J.D., Impey, R.W., & Klein, M.L. (1983) *J. Chem. Phys.* **79**, 926–935.
21. Feller, S.E., Zhang, Y.H., Pastor, R.W., & Brooks, B.R. (1995) *J. Chem. Phys.* **103**, 4613–4621.